

Microring-based modulation and demodulation of DPSK signal

Lin Zhang^{1*}, Jeng-Yuan Yang¹, Muping Song^{1,2}, Yunchu Li¹, Bo Zhang¹, Raymond G. Beausoleil³, and Alan E. Willner¹

¹Department of Electrical Engineering, University of Southern California, Los Angeles, CA 90089, USA

²Department of Information and Electronic Engineering, Zhejiang University, Hangzhou, Zhejiang, 310027, China

³HP Laboratories, Palo Alto, CA 94304, USA

*Corresponding author: linzhang@usc.edu

Abstract: Ultra-small modulator and demodulator for 10 Gb/s differential phase-shift-keying (DPSK), using silicon-based microrings, are proposed. A single-waveguide microring modulator with over-coupling between ring and waveguide generates a DPSK signal, while a double-waveguide microring filter enables balanced DPSK detection. These modulator and demodulator are characterized. A trade-off between pattern dependence of the Duobinary signal and alternate-mark inversion signal power in demodulator design is discussed. Power penalty of the proposed approach is 0.8 dB relative to baseline using conventional modulation and demodulation techniques.

©2007 Optical Society of America

OCIS codes: (060.0060) Fiber optics and optical communications; (130.0130) Integrated optics; (200.4650) Optical interconnects; (230.4110) Modulators; (999.9999) Silicon photonics.

References and links

1. A. H. Gnauck, and P. J. Winzer, "Optical phase-shift-keyed transmission," *J. Lightwave Technol.* **23**, 115-130 (2005).
2. E. A. Swanson, J. C. Livas, and R. S. Bondurant, "High sensitivity optically preamplified direct detection DPSK receiver with active delay-line stabilization," *IEEE Photon. Technol. Lett.* **6**, 263-265 (1994)
3. E. Ciaramella, G. Contestabile, and A. D'Errico, "A novel scheme to detect optical DPSK signals," *IEEE Photon. Technol. Lett.* **16**, 2138-2140 (2004)
4. I. Lyubomirsky and C. Chien, "DPSK demodulator based on optical discriminator filter," *IEEE Photon. Technol. Lett.* **17**, 492-494 (2005)
5. L. Christen, Y. K. Lize, S. Nuccio, J.-Y. Yang, S. Poorya, A. E. Willner, L. Paraschis, "Fiber Bragg grating balanced DPSK demodulation," in *Proceedings of IEEE LEOS Annual Meeting 2006* (Institute of Electrical and Electronics Engineers, Montreal, Canada, 2006), pp. 563-564.
6. D. A. B. Miller, "Optical interconnects to silicon," *IEEE J. Sel. Top. Quantum Electron.* **6**, 1312-1317 (2000).
7. C. A. Barrios and M. Lipson, "Modeling and analysis of high-speed electro-optic modulation in high confinement silicon waveguides using metal-oxide-semiconductor configuration," *J. Appl. Phys.* **96**, 6008-6015 (2004)
8. R. D. Kekatpure and M. L. Brongersma, "CMOS compatible high-speed electro-optical modulator," *Proc. SPIE* **5926**, paper G1 (2005)
9. Q. Xu, B. Schmidt, S. Pradhan, and M. Lipson, "Micrometre-scale silicon electro-optic modulator," *Nature* **435**, 325-327 (2005)
10. C. A. Barrios, "Electrooptic modulation of multisilicon-on-insulator photonic wires," *J. Lightwave Technol.* **24**, 2146-2155, (2006)
11. Y. Chen and S. Blair, "Nonlinear phase shift of cascaded microring resonators," *J. Opt. Soc. Am. B*, **20**, 2125-2132 (2003)
12. J. E. Heebner, V. Wong, A. Schweinsberg, R. W. Boyd, and D. J. Jackson, "Optical transmission characteristics of fiber ring resonators," *IEEE J. Quantum Electron.* **40**, 726-730 (2004)
13. A. Stapleton, S. Farrell, H. Akhavan, R. Shafiiha, Z. Peng, S.-J. Choi, J. O'Brien, P. D. Dapkus, and W. Marshall, "Optical phase characterization of active semiconductor microdisk resonators in transmission," *Appl. Phys. Lett.* **88**, 031106 (2006)
14. R. A. Soref, B. R. Bennett, "Electrooptical effects in silicon," *IEEE J. Quantum Electron.* **23**, 123-129 (1987)
15. B. E. Little, S. T. Chu, H. A. Haus, J. Foresi, and J.-P. Laine, "Microring resonator channel dropping filters," *J. Lightwave Technol.* **15**, 998-1005 (1997)

1. Introduction

Advanced data modulation formats have become quite important within the optical communications community, and of particular interest is differential-phase-shift-keying (DPSK) [1]. When compared to amplitude-shift-keying, DPSK exhibits a 3-dB increase in receiver sensitivity and is more tolerant to fiber nonlinearities [1]. DPSK signal, which carries information via the phase difference of adjacent symbols, is typically modulated using either a phase modulator or Mach-Zehnder modulator (MZM) [1], while a delay-line interferometer (DLI) is used as a demodulator for balanced detection [2]. More recently, several novel demodulation schemes have been reported [3-5]. But these modulators and demodulators are relatively complicated, which causes higher cost of DPSK transmitter and receiver. Moreover these devices are fairly large, on the order of a centimeter, which may mean large power consumption.

Micro-ring based devices have attracted a great deal of attention in recent years. Silicon-based microring modulators, switches and filters, fabricated in silicon-on-insulator (SOI) platform, have been demonstrated [7-9]. But, to our knowledge, there is no report to use microring-based devices to generate and demodulate DPSK signals.

We propose using integrated ring resonator structures to (de)modulate DPSK signals, which replace the interferometers for DPSK-based communication and interconnect systems. As compared to conventional MZMs and DLIs, microring structures require a relatively small chip area and low driving power, and are easy to fabricate into arrays.

In this paper, we numerically outline and analyze the use of the π phase shift from a ring resonator to generate DPSK as well as using a ring resonator surrounded by two waveguides to achieve a DLI-type filtering function for demodulation. A trade-off between data pattern dependence of the Duobinary signal and power loss of the alternate-mark inversion (AMI) signal is identified, as cavity Q-factor of the demodulator varies. Power penalty is diminished to 0.8 dB with an optimal cavity Q-factor of 22000 for 10 Gb/s non-return-to-zero (NRZ) DPSK, which is relatively low compared to some published demodulation schemes.

2. Principle

Typically, DPSK is generated by using a MZM to introduce a π phase shift between bits if the sign of the second bit is meant to flip from a "1" to "0" from the first bit. Phase shift of π is realized across the minimum point of transfer function of a MZM, which causes intensity dips in modulated signals. An alternative way to modulate DPSK can be direct phase modulation, which induces undesired frequency chirp.

Microring modulators were demonstrated only for intensity modulation by switching output optical power on and off through shifting of the ring resonance peak. This shifting can be realized by varying carrier density and thus refractive index in the ring cavity, when a voltage is applied or carriers are injected. In the electrical domain, the microring modulators are typically based on MOS capacitors [7-8] or p-i-n diodes [9]. Many novel structures and driving schemes have already been proposed to increase modulation speed and efficiency [10]. Here a MOS-capacitor-based modulator is considered since it is more suitable for high-speed operations. In the optical domain, a microring in a single-waveguide configuration can be over-coupled (i.e., waveguide-ring coupling > ring loss), causing phase shift of 2π across resonance [11-13]. In this case, the transfer function of the over-coupled ring is obtained from

$$\frac{E_{out}}{E_{in}} = \frac{t - a \exp(i\phi)}{1 - ta \exp(i\phi)} \quad (1)$$

where t and a stand for the transmission coefficient and loss, and ϕ is phase change in one round trip [11]. When the resonance peak is shifted, the continuous wave (CW) laser source can experience a phase shift of π across the center of the phase profile, as shown in Fig. 1(a), and have the same power in each bit duration. NRZ DPSK data format is generated this way. It is important to note that there are intensity dips at bit transitions in the modulated signal, which are caused by the notched profile of the ring resonator (see Fig. 1(a)). On the other

hand, when the resonance profile is moved, the optical signal also experiences a fast phase shift, which will give rise to frequency chirp at the bit transitions. A major difference between our microring-based DPSK modulator and a conventional phase modulator or MZM is that there are both intensity dips and frequency chirp in the modulated signal.

To model the behavior of the microring-based silicon modulators, an ideal 10 Gb/s NRZ drive voltage is sent through a five-pole Bessel electrical filter so that drive pulses have rise and fall times of ~10 ps [10]. As a simplified model, variation in carrier density is simulated as a charging process following the applied voltage, which is believed to be a good fit to real behavior in MOS capacitors [8]. The carrier transit time, defined as the duration for carrier density to increase from 10% to 90% of its peak value when a voltage step is applied, is considered here from 12 to 50 ps [7, 10]. Transit time is set to be the same at rising and falling edges, which is a reasonable approximation in many MOS-capacitor designs [10]. Refractive index is then calculated from the carrier density [14], and the ring resonance peak is shifted according to the waveform of the refractive index. Change in voltage from 0 to 2.2 V causes a resonance peak shift of 0.08 nm towards shorter wavelength. Continuous wave from laser source is then modulated. The ring resonator, with a radius of 5 μm, has cavity Q-factor of 10000. A set of dynamics equations given in Ref. [15] is numerically solved to obtain the modulated signals, in which photon lifetime of ring resonators is considered.

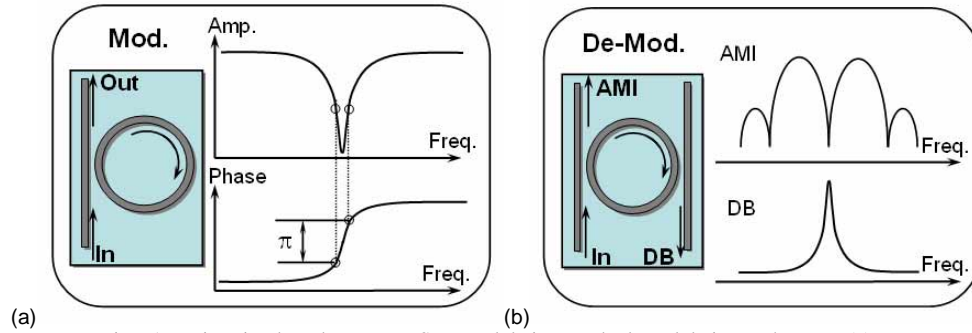


Fig. 1. Microring-based NRZ-DPSK modulation and demodulation schemes. (a) In modulation, CW experiences a phase shift of π between two open circles, using a single-waveguide over-coupled structure. (b) Demodulation is achieved using a double-waveguide microring filter where Duobinary and AMI are obtained in the band-pass and notch ports.

Demodulation of DPSK signals can be achieved using a single-ring double-waveguide filter, as shown in Fig. 1(b), in which one output port works as a band-pass filter to obtain the Duobinary signal, and the other as a notch filter to produce the AMI signal. The transfer function of the microring filter can be derived [11], as shown below,

$$\frac{E_{out}}{E_{in}} = \frac{(1-t^2)\sqrt{a}\exp(i\phi)}{1-t^2a\exp(i\phi)} \quad (2)$$

where t , a and ϕ are defined as before. This microring filter actually functions as a discriminator to convert the phase-modulated signal to amplitude-modulation for direct detection [4-5]. Duobinary and AMI are detected individually and then combined electrically to obtain balanced detection of DPSK signal.

3. Results

We first plot the symbol constellation diagram for the proposed DPSK modulation scheme, in which the electric field of the modulated optical wave is mapped into the complex plane, as shown in Fig. 2(a). The microring-based DPSK modulator (dash) is compared to those obtained from phase modulator (dash dot) and MZM (dot). Frequency chirp will occur unless the modulated optical field transits between two symbols (black dots) exactly along the real axis, so only a MZM can produce a chirp-free signal. On the other hand, the intensity dip at a bit transition can be removed only when the transition between the two symbols is along an arc, like those created by a phase modulator [1]. From Fig. 2(a), we note that the microring-

based DPSK modulator induces both frequency chirp and intensity dips. But fortunately, the frequency chirp and intensity dips always occur together meaning that the chirp is at low power. The DPSK signal modulated with microring has a transition close to the real axis making it very similar to that of a MZM. This is verified in Fig. 2 (b), in which -3 and -10 dB signal bandwidths are examined as a function of transit time. For a long transit time, signal bandwidth can be narrower, compared to a MZM. Spectra of a MZM and a microring modulator are plotted with the same scale (10 dB/div. in power and 20 GHz/div. in frequency) in Fig. 2 (c) and (d), when the carrier transit time is 16 ps. We note that the microring-based DPSK modulation produces a spectrum very similar to that given by the MZM, although it is a little broader in the low-power regions far away from signal carrier due to the chirp. Since the intensity dips keep the frequency chirp at low power levels, the chirp-induced spectrum broadening is small.

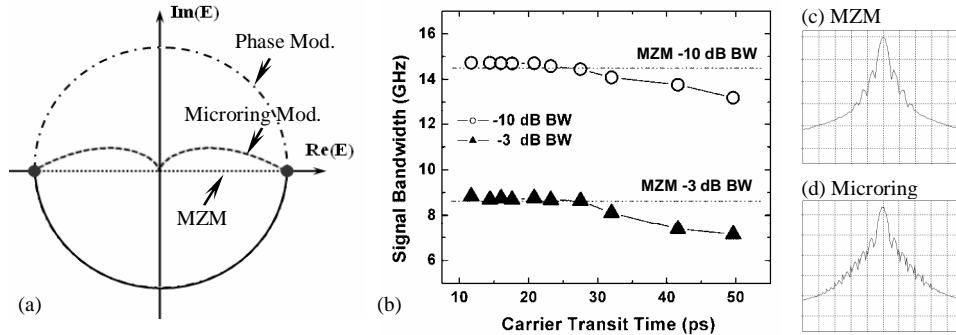


Fig. 2. (a) Symbol constellation diagrams for microring-based modulator (dash), phase modulator (dash dot) and MZM (dot). (b). DPSK signal bandwidth vs. transit time. (c). DPSK spectrum modulated by MZM. (d). DPSK spectrum modulated by microring, in the same scale. (10 dB/div. in power and 20 GHz/div. in frequency)

To evaluate the performance of the microring-based DPSK modulator, a DLI-based demodulator is used to isolate the effects of the modulator on signal quality. Fig. 3(a) shows eye-opening penalty, compared to a MZM, as a function of transit time. We consider a well-biased case, in which the resonance peak is shifted by 0.08 nm, and CW carrier is originally located 0.04-nm away from the resonance peak. Modulated signal has the same maximum transmission, as shown in Fig. 1(a). The eye-opening penalty increases with transit time. In Fig. 3(a) eye-diagrams are shown in the same scale and correspond to transit times of 16 and 50 ps, respectively. Tracks in the eye-diagrams split at long transit time because the refractive index at for a single '1'-bit has a smaller modulation depth, compared to consecutive '1'-bits, and thus the maximum transmission is not reached for a single '1'-bit. Timing jitter in the modulated signal also becomes worse as seen in the eye-diagrams. Nevertheless, the microring-based modulator can produce good DPSK signals with no visible imperfections, as long as the transit time is shorter than 30 ps, which can be easily achieved [7,10].

Modulation performance is examined for different bias conditions. CW offset, defined as $(\lambda_{\text{resonance}} - \lambda_{\text{CW}}) - 0.04\text{nm}$, is set from 0 to 0.016 nm. As shown in Fig. 3(b), the eye-opening penalty almost linearly increases with CW offset. Data quality is degraded by '1'-level splitting in the modulated signal, with an almost unchanged '0'-level, as shown in eye-diagrams in Fig. 3(b). Time jitter in the modulated signal is more severe. Compared to Fig. 3(a), it is noted that the bias condition is more critical to keep good modulation performance.

To demodulate a DPSK signal, the microring-based double-waveguide filter is used to extract Duobinary and AMI signals from the DPSK by spectrum slicing. The micro-ring demodulator has a cavity Q-factor of up to 25000 and a radius of 5 μm . A MZM is used as a DPSK modulator to isolate effects of the demodulator. First, we examine whether or not correct data pattern is demodulated by the spectrum-slicing scheme, because it may cause a clean eye-diagram but incorrect information. For example, if a two-bit-time DLI is used, which functions as a periodic spectrum slicer with a FSR of the half bit-rate, then good eye-

diagrams can be obtained, but the demodulated information is not the same as what is modulated and must be post-coded to retrieve the correct data.

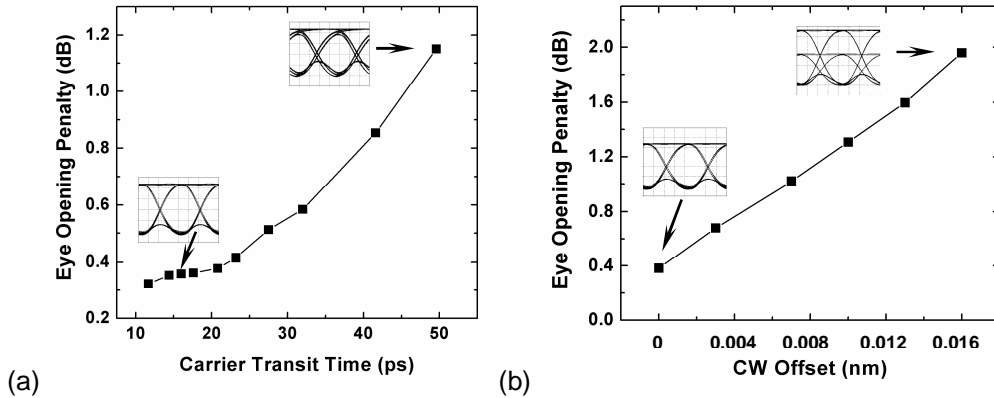


Fig. 3. Eye-opening penalty of the modulated DPSK signal, compared to a MZM, versus carrier transit time (a) and CW offset (b). Two eye-diagrams in each figure are shown in the same scale.

Figure 4 shows original logic data bits that are then pre-coded and modulated onto a CW carrier. We note that the demodulated Duobinary and AMI signals contain the correct data pattern. It can be seen that, in the Duobinary signal, optical power rises, but this happens only between adjacent '0'-bits, which will not be sampled in signal detection. This means that a microring-based filter can be used as a DPSK demodulator in principle.

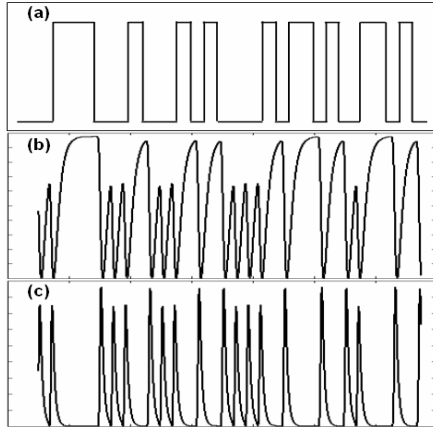


Fig. 4. A comparison of original logic (a), obtained Duobinary (b) and AMI (c) data shows correct information is demodulated.

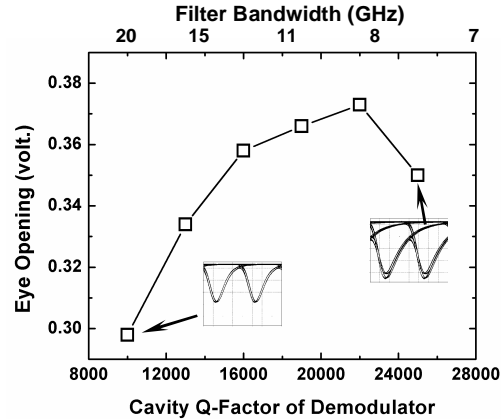


Fig. 5. Quality of the demodulated signal is examined with varied cavity Q-factor. Two eye-diagrams are shown in the same scale.

As a key parameter, cavity Q-factor of the microring-based demodulator is optimized. As shown in Fig. 5, using MZM as DPSK modulator, eye-opening of the demodulated signals increases with the Q-factor and reaches the maximum when $Q=22000$. This is attributed to the fact that, when Q-factor is higher, the notch filter profile of the demodulator becomes narrower and leaves more power in the AMI port. Since optical power of the AMI signal is increased, the eye-diagram is more open in balanced detection, as seen from the eye-diagrams for Q-factors of 10000 and 25000 in Fig. 5. However, correspondingly, the Duobinary signal is cut by the narrowed bandpass filtering, which causes pattern dependence in the Duobinary data. A single '1'-bit has a lower instantaneous power than consecutive '1'-bits at the sampling instant, as shown in the eye-diagrams, and this may decrease eye-opening with Q-factor higher than 22000. The trade-off between AMI signal power and Duobinary data pattern dependence originates from the Lorentzian shape of micro-ring resonance.

Comparatively, a traditional DLI has a cosine-squared filter shape for its transfer function. The micro-ring DPSK demodulator has to have a balance between keeping AMI power and maintaining the Duobinary spectrum. An optimal cavity Q-factor is chosen to be 22000, and beyond this, eye-opening drops due to the pattern dependence in the Duobinary data.

Figure 6 shows the tolerance of demodulation performance to varied signal bit-rate. DPSK signal is generated by a MZM, and a microring-based DPSK demodulator with Q-factor of 22000 is compared to a DLI that is designed for 10 Gb/s DPSK signal. Eye-opening penalty is caused when the bit-rate is changed away from 10 Gb/s. We note that the microring demodulation scheme exhibits better tolerance to a lowered bit-rate, while it induces a larger penalty than a DLI, for an increased bit-rate, which is because the Duobinary signal suffers very much from the pattern dependence. In fact, optimal cavity Q-factor in demodulation for 10 Gb/s DPSK is between 19000 and 22000 but very near 22000. Thus, when the cavity Q-factor is fixed at 22000, 9 Gb/s signal shows a better demodulation performance.

Employing microring structures as both the modulator and demodulator, overall performance of a DPSK link is examined for the back-to-back case and compared to using regular MZM and DLI. Transit time in the modulator is set to be 16 ps, and Q-factor in the demodulator is chosen to be 22000, in a well-biased case. With receiver sensitivity of -25 dBm, BER curves are plotted in Fig. 7. Error-free detection can be easily achieved by increasing received power, with a power penalty of about 0.8 dB between the microring-based and traditional scheme. As described above, this penalty comes mainly from non-ideality of the microring-based demodulator and is expected to be decreased further by improving the ring structure in the future.

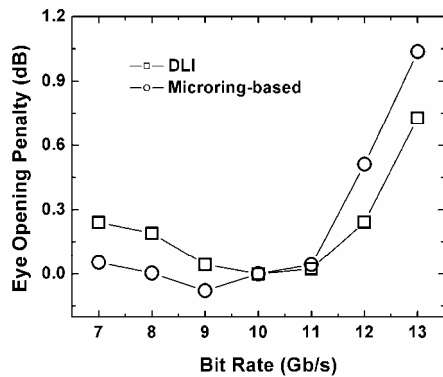


Fig. 6. Tolerance of microring-based DPSK demodulator and DLI to varied signal bit-rate. The proposed approach is more tolerant to a lowered bit rate.

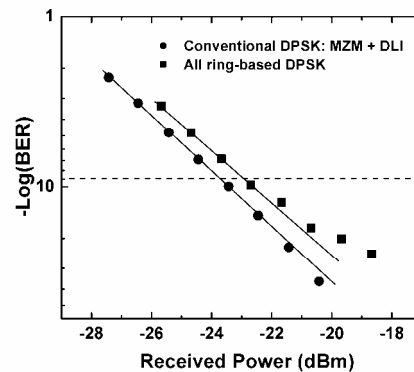


Fig. 7. BER curves given by all microring-based DPSK modulation and demodulation, with 0.8-dB power penalty, compared to a conventional DPSK link: MZM + DLI.

4. Conclusion

We have proposed silicon microring-based modulation and demodulation of DPSK signals, which enables integrated ultra-small DPSK transmitters and receivers. Single-waveguide microring modulator with over-coupling is used to achieve a phase shift of π , and eye-opening penalty can be as low as 0.35 dB, compared to a MZM. Demodulation of a DPSK signal has been realized using a double-waveguide microring filter, which extracts the Duobinary and AMI formats from the DPSK spectrum simultaneously for balanced detection. Low power penalty of 0.8 dB is achieved by optimizing cavity Q-factor of the microring filter. A trade-off between pattern dependence of Duobinary signal and power loss of AMI signal is identified.

Acknowledgments

The authors would thank Dr. Gunn, Rohan Kekatpure, and Dr. Preble for their helpful discussions. This work is sponsored by Army Nanophotonics program and DARPA UNIC program.